

Determination of the Binding Specificity of an Integral Membrane Protein by Saturation Transfer Difference NMR: RGD Peptide Ligands Binding to Integrin $\alpha_{IIb}\beta_3$ [†]

Robert Meinecke and Bernd Meyer*

Institute for Organic Chemistry, University of Hamburg, Martin Luther King Pl. 6, 20146 Hamburg, Germany

Received May 2, 2001

Saturation transfer difference (STD) NMR is a fast and versatile method to screen compound mixtures in the presence of a receptor for binding affinity and to characterize the ligand's binding epitope. Here we demonstrate that ligand interactions with integral membrane proteins can be investigated by STD NMR if the receptor is embedded into the lipid bilayer of a liposome. The integrin $\alpha_{IIb}\beta_3$, also termed GPIIb-IIIa, is a platelet surface glycoprotein that plays a pivotal role in platelet aggregation and that interacts with proteins and peptides presenting the peptide recognition motif RGD. Purified human integrin $\alpha_{IIb}\beta_3$ was incorporated into liposomes, and the binding of RGD peptides was analyzed by STD NMR techniques. Cyclo(RGDfV) gave STD NMR effects in the presence of liposomes containing the integrin. The magnitude of the STD effect as a function of the ligand's concentration gave a value for the dissociation constant of 30–60 μ M. Adding the weakly binding RGD to the solution of cyclo(RGDfV) resulted in STD effects of the stronger ligand cyclo(RGDfV) only. This demonstrates in agreement with literature that the peptide RGD is a much weaker ligand to the integrin than the peptide cyclo(RGDfV) that largely replaces the RGD peptides from the binding site. The binding epitope of the ligand cyclo(RGDfV) was characterized by STD NMR to contain sections of the D-Phe, the Val methyl groups, Arg α , β , and γ protons, one H β of Asp, and one H α of Gly.

Introduction

In contrast to soluble proteins, there is comparatively little information available about ligand–receptor interactions that occur at membrane surfaces. Most of the biomedical relevant proteins are membrane-bound; as an example, about 7% of the human genome is coding for seven helix trans membrane receptors. However, handling is problematic, because the aggregation behavior of membrane proteins is unpredictable. Sometimes a truncated, soluble form of the receptor is accessible, but the binding affinity or binding specificity of this form may differ from the native receptor properties that is embedded into a membrane. The biophysical environment of a membrane is considerably different from the isotropic extracellular medium. Parameters that drastically change are the ionic strength, the ion composition, and the electric field strength. It is therefore desirable to investigate membrane proteins as the integrin $\alpha_{IIb}\beta_3$ and their binding specificity directly in living cells or at least in reconstituted membrane systems (cf. Figure 1).

Receptor proteins are involved in numerous binding interactions. Many NMR methods have been developed to screen and to characterize binding processes, e.g.,

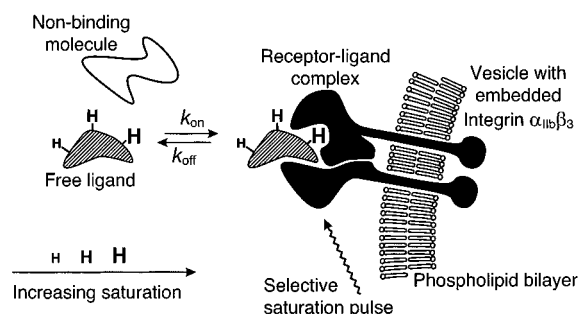


Figure 1. On the right, a heterodimeric integrin $\alpha_{IIb}\beta_3$ molecule is shown schematically reconstituted in a liposome also called large unilamellar vesicle (LUV). The protein molecules are randomly inserted into the lipid bilayer so that only half of the binding sites are pointing outside and are accessible to ligands in the buffer solution. Ligand binding is detected with STD NMR spectroscopy. Saturation of the receptor is achieved by selective irradiation within 100 ms. The saturation is transferred to bound ligands via intermolecular spin diffusion. The effect of the saturation is made visible by subtracting the spectrum with protein saturation from one where the receptor has not been saturated. Signals of nonbinding molecules are canceled out by subtraction. Ligand protons in close proximity to the protein receive larger saturation and thereby reveal the ligand's binding epitope.

[†] Abbreviations: integrin $\alpha_{IIb}\beta_3$ fibrinogen receptor, platelet glycoprotein IIb-IIIa; cyclo(RGDfV), cyclo(1,5)-arginyl-glycyl-aspartyl-D-phenylalanyl-valine; DMPC, 1,2-dimyristoyl-*rac*-glycero-3-phosphocholine; DMPG, 1,2-dimyristoyl-*sn*-glycero-3-[phospho-*rac*-(1-glycerol)] sodium salt; LUV, large unilamellar vesicles; PAGE, polyacrylamide gel electrophoresis; RGD, arginyl-glycyl-aspartic acid; SDS, sodium dodecyl sulfate; SAR, structure–activity relationship; STD, saturation transfer difference; trNOE, transferred nuclear Overhauser effect.

* To whom correspondence should be addressed. Tel: +49 40 42838 5913. Fax: +49 40 42838 2878. E-mail: Bernd.Meyer@sg11.chemie.uni-hamburg.de. Web: <http://sg11.chemie.uni-hamburg.de>.

trNOE spectroscopy,^{1–3} SAR by NMR,⁴ and NOE pumping.⁵ Recently, we published the STD NMR method that offers several advantages over other bioaffinity assays.^{6,7} Compounds with binding affinity to a receptor can directly be identified from a substance mixture allowing STD NMR to be used as a screening method. The basis for STD NMR is the transfer of saturation from the protein to the ligand. Selective saturation of the protein

is possible because protein signals are often anisotropically shifted and broadened and can be irradiated outside the spectral window of low molecular weight compounds. In macromolecules, dipolar coupling of proton spins is extremely efficient because of restricted molecular mobility. Through spin diffusion the magnetization is spread over the entire protein within less than 0.1 s. This saturation of the protein is transferred to bound ligands by intermolecular spin diffusion (cf. Figure 1). The signals of the ligands are made visible by subtracting the saturated spectrum from one without protein saturation. In this difference spectrum, signals of nonbinding molecules are canceled out by subtraction. Saturated resonances of ligand molecules are detected in the free state. Using this information, the biologically active components can be identified from a mixture of compounds. Additionally, the ligand's binding epitope can be determined from the spectra because protons in close proximity to the protein in the binding site carry a much larger saturation than the others that obtain saturation only through spin diffusion within the ligand.⁸ Detecting binding affinity by STD is a very sensitive NMR method that usually works with less than 1 nmol of protein. The ligand is supplied in a large excess. There is no upper limit of receptor size, and ligand excess is not critical. STD NMR is therefore well suited for the analysis of liposome-bound receptors.

The integrin $\alpha_{IIb}\beta_3$, often referred to as GP IIb-IIIa or fibrinogen receptor, is the most abundant platelet cell surface glycoprotein and consists of the two non-covalently linked α and β subunits of MW = 125 kDa and MW = 108 kDa, respectively.^{9–12} The dimerization is calcium-dependent. In the activated state, the integrin binds to fibrinogen and mediates thrombus formation by platelet aggregation. As recognition sites, the peptide sequences RGDS (α chain residues 572–575),¹³ RGDF (α chain residues 95–98),¹⁴ and HHLGGAK-QAGDV (γ chain residues 400–411)¹⁵ have been localized in fibrinogen. The RGD sequence is recognized by the integrin $\alpha_{IIb}\beta_3$ as part of proteins and as short linear peptides.¹⁶ Other extracellular matrix proteins such as fibronectin, vitronectin, thrombospondin, and von-Willebrand-factor also bind to integrin $\alpha_{IIb}\beta_3$. A related cellular receptor, the integrin $\alpha_v\beta_3$, has similar binding preferences. It was shown that conformational restrictions of the RGD segment can induce significant selectivity for the integrin $\alpha_v\beta_3$. By optimizing selectivity of cyclic RGD-containing pentapeptides for the integrin $\alpha_v\beta_3$, cyclo(RGDfV) has been developed by Kessler and co-workers.^{17,18} This cyclic peptide also strongly binds to the integrin $\alpha_{IIb}\beta_3$. In competition assays, Pfaff et al.¹⁹ found a $K_D = 5.05 \mu\text{M}$ as the dissociation constant of $\alpha_{IIb}\beta_3$ embedded in planar lipid bilayers. Keenan et al.²⁰ applied a different competitive binding assay and determined $K_i = 42 \mu\text{M}$ for the binding affinity of liposome-incorporated $\alpha_{IIb}\beta_3$ to cyclo(RGDfV). For inhibition of fibrinogen binding to immobilized $\alpha_{IIb}\beta_3$, the IC_{50} value of cyclo(RGDfV) is $29 \mu\text{M}$; and with octyl-glucoside-solubilized $\alpha_{IIb}\beta_3$, the IC_{50} is 230 nM (ELISA).¹⁹ Another solid-phase assay employing the inhibition of biotinylated solubilized $\alpha_{IIb}\beta_3$ binding to immobilized fibrinogen gave an IC_{50} of $12 \mu\text{M}$ for cyclo(RGDfV).¹⁷ It follows that the dissociation constant for cyclo(RGDfV) binding to integrin $\alpha_{IIb}\beta_3$ is in the low micromolar range.

Materials and Methods

The liposomes were prepared according to a modified procedure of Gerritsen et al.²¹ and Müller et al.²² In a glass vial, $3.39 \mu\text{mol}$ (2.30 mg) of 1,2-dimyristoyl-*rac*-glycero-3-phosphocholine (DMPC) in $230 \mu\text{L}$ of chloroform and 348 nmol ($240 \mu\text{g}$) of 1,2-dimyristoyl-*sn*-glycero-3-[phospho-*rac*-(1-glycerol)] sodium salt (DMPG) in $24 \mu\text{L}$ of chloroform/methanol 2:1 (v/v) were deposited as a thin film by rotation under a stream of nitrogen and dried under vacuum for 8 h. For all preparations a LUV-NMR buffer was used that consists of deuterium oxide (D_2O 99.9%), 10 mM perdeutero tris(hydroxymethyl)aminomethane (TRIS-d_{11}), 10 mM NaCl, and 6 mM NaN_3 and is adjusted to pD 7.4 with 100 mM DCl in D_2O . The lipid film was solubilized in 3.37 mL of LUV-NMR buffer by adding $47 \mu\text{L}$ of 100 g/L Triton X-100, and sonification for 45 min at 4°C . Then $88 \mu\text{L}$ of 20 mM CaCl_2 in D_2O and 1 mg of human integrin (Calbiochem-Novabiochem Corporation, USA) $\alpha_{IIb}\beta_3$ in 200 μL of LUV-NMR buffer containing additionally 1 g/L Triton X-100 and 0.5 mM CaCl_2 were added to the solubilisate at 4°C . The mixture was gently agitated at 37°C for 1 h. Bio-Beads SM-2 (Bio-Rad Laboratories, USA) were washed with methanol and H_2O .²³ After rinsing in D_2O and equilibration in LUV-NMR buffer containing additionally 0.5 mM CaCl_2 , 360 mg of wet Bio-Beads SM-2 were added to the mixed solubilisates and agitated at 26°C for 2 h. The liquid was separated from the Bio-Beads, and the adsorption step was repeated once in a new vial, but the amount of SM-2 beads was reduced to 80 mg. For NMR measurements, the liposomes were concentrated to a final volume of 500 μL or 200 μL using a Ultrafree-4 ultrafiltration tube (100 kDa PES membrane, Millipore Corporation, USA).

Prior to LUV preparation, the integrin $\alpha_{IIb}\beta_3$ supplied in 270 μL of H_2O /glycerol 1:1 (v/v) buffer had been diluted with 1.8 mL of LUV-NMR buffer containing additionally 0.3 g/L Triton X-100 and 0.5 mM CaCl_2 . A Centricon-10 ultrafiltration tube (Millipore Corporation, USA) was used for concentration to a final volume of 200 μL . For complete buffer exchange, the diluting and concentration steps were repeated five times. NMR samples were prepared in standard tubes or in Advanced NMR Microtubes (12 mm bottom, Shigemi Co. LTD, Japan). Peptide ligands were purchased (Bachem, Germany).

All NMR experiments were performed at a temperature of 283 K on a Bruker Avance DRX 500 MHz spectrometer equipped with a 5 mm inverse triple resonance probe head. Selective saturation of the protein was achieved by a train of Gauss-shaped pulses of 50 ms length each, separated by a 1 ms delay. A number of 40 or 20 selective pulses was applied, leading to a total length of the saturation train of 2.04 or 1.02 s. The on-resonance irradiation of the protein was performed at a chemical shift of 12 ppm or -1 ppm . Off-resonance irradiation was set at 80 or 160 ppm, where no protein signals were present. The spectra were subtracted internally via phase cycling after every scan to minimize artifacts arising from temperature and magnetic field instability. Total scan number in STD experiments was 8–12K; in normal spectra without applying STD, it was 1K. NMR spectra were multiplied by an exponential line broadening function of 1.0–2.0 Hz prior to Fourier transformation. All spectra were recorded using 10 ppm spectral width and a 20–80 ms spin lock pulse which eliminates the background protein resonances. Spectra processing was performed on Silicon Graphics O_2 workstations using Xwinnmr 2.5 software (Bruker).

Results

Here we present the application of STD NMR analysis of binding of ligands to the interaction between a liposome integrated membrane protein and peptide ligands. As shown in Figure 1, saturation is transferred from the membrane-bound receptor to ligands when the ligand binds to the protein. Because the protein is integrated into the membrane, a very efficient satura-

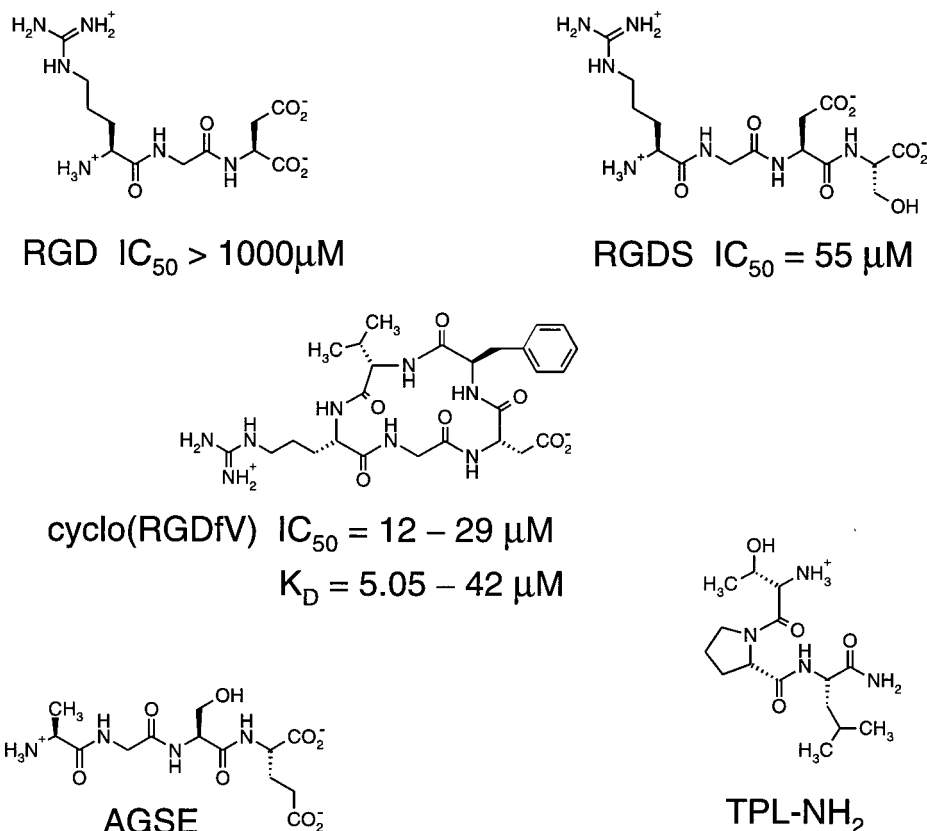


Figure 2. RGD-peptides with binding affinity to integrin $\alpha_{\text{IIb}}\beta_3$, i.e., RGD, RGDS, and cyclo(RGDfV), as well as peptides without binding affinity, i.e., AGSE and TPL-NH₂. The inhibitory effects of RGD and RGDS on fibrinogen binding to activated platelets that present the integrin were investigated by Tranqui et al.²⁹ The IC_{50} values (ELISA) and the dissociation constants of cyclo(RGDfV) were determined by Aumailley et al.,¹⁷ Pfaff et al.,¹⁹ and Keenan et al.²⁰

tion of the protein is possible due to the slow tumbling of the liposome. Through exchange between free and bound state, the saturation of the ligand is transferred to solution, where it is detected. By application of difference spectroscopy, signals of nonbinding molecules are canceled out. The STD NMR spectra allow identification of binding and characterization of the binding epitopes on the ligands.^{6,8} We prepared the liposomes according to a modified procedure of Gerritsen et al.²¹ and Müller et al.²² In a liposome suspension, small peptide ligands show an NMR line width of 2–3 Hz. Line-broadening effects of susceptibility discontinuities and dipolar coupling are not significantly contributing to the line width, and hence no MAS conditions are necessary to obtain a high resolution NMR spectrum. Liposomes were prepared from detergent solubilized phospholipids DMPC and DMPG in a molar ratio of 10:1 with the solubilized integrin. Vesicles form spontaneously if detergent is withdrawn from the equilibrium by adding a selective adsorbent. The protein is statistically oriented with its binding site pointing outward or pointing into the liposome such that only 50% of the binding sites are accessible to the ligands in solution. It was shown that such liposomes have an average diameter of 200 nm.²⁴ Assuming an area of 0.7 nm^2 ($7 \times 10^{-19}\text{ m}^2$) per phospholipid molecule,²⁵ a 900-fold initial molar excess of lipid over integrin and a receptor recovery of 50% due to loss during incorporation,²² liposomes result that consist of approximately 360 000 lipid molecules and 200 receptors. This is equivalent to 1800 lipid molecules per receptor. Without the enclosed

water, the total molecular weight of the vesicles is 290 MDa and the protein fraction is ~16%.

To analyze binding to the now membrane integrated integrin, we used several peptide derived ligands with known binding property to the receptor. As negative controls we used nonbinding peptides with the integrin containing liposomes. As a further negative control, integrin ligands were used with liposomes that were prepared in the same fashion but without the protein added to test for unspecific interactions of the peptides with the phospholipid bilayer itself.

Binding of Cyclo(RGDfV) to Integrin $\alpha_{\text{IIb}}\beta_3$. The ligand cyclo(RGDfV) (cf. Figure 2) has a known binding specificity to integrins $\alpha_{\text{IIb}}\beta_3$ and $\alpha_v\beta_3$.¹⁸ Its binding constant to $\alpha_{\text{IIb}}\beta_3$ was determined to be $\text{IC}_{50} = 12\text{--}29\mu\text{M}$.^{17,19} Adding cyclo(RGDfV) to a liposome preparation of the integrin $\alpha_{\text{IIb}}\beta_3$ resulted in STD signals of the cyclopeptide (cf. Figure 3). Figure 3a shows a normal 1D ^1H NMR spectrum of the mixture of cyclo(RGDfV) and the liposomes containing integrin. Figure 3b,c shows the STD spectra of the mixtures of integrin containing liposomes with a 6-fold and a 55-fold excess of the cyclopeptide, respectively. Here, the intensity of the cyclo(RGDfV) signals increases strongly with a larger excess of the ligand.

The titration curve of the integrin containing liposomes with the cyclopeptide is shown in Figure 4. The concentration of the protein was $5\mu\text{M}$, and the excess of the ligand varies from 6-fold to 55-fold equivalent to concentrations from 29 to $275\mu\text{M}$, respectively. The change of the relative integral of three representative

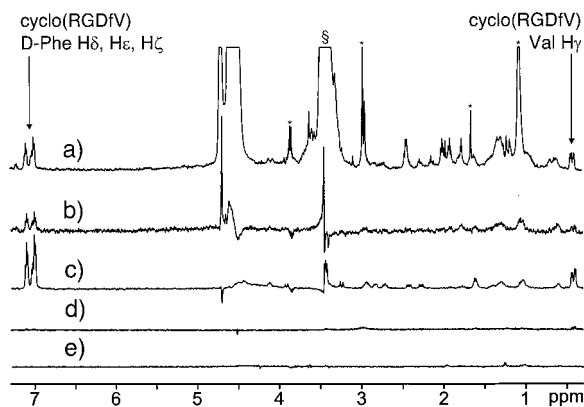


Figure 3. (a) Normal ¹H NMR spectrum of 29 μM cyclo(RGDfV) and integrin α_{IIb}β₃ liposomes showing signals of the ligand and residual protein resonances. (S TRIS buffer; * impurities). (b) STD NMR spectrum of 29 μM cyclo(RGDfV) and integrin α_{IIb}β₃ containing liposomes showing STD effects of the ligand. (c) Same as b but 275 μM cyclo(RGDfV) showing the increase of the STD signals with ligand excess. (d) STD NMR spectrum of 260 μM cyclo(RGDfV) and 260 μM RGD with liposomes devoid the integrin receptor showing no unspecific binding to the liposomes. (e) STD NMR spectrum of 160 μM AGSE and integrin α_{IIb}β₃ containing liposomes. The nonbinding peptide shows no STD effects.

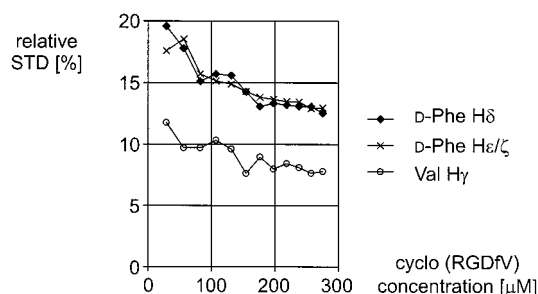


Figure 4. Titration of cyclo(RGDfV) into a solution containing the liposome embedded integrin α_{IIb}β₃. The concentration of the protein was 5 μM, and the concentration of the ligand varies from 29 μM to 275 μM. The relative STD effects of the three signals from Phe Hδ, Hε/Hζ, and Val Hγ are shown. This effect is defined by dividing the integral of the STD signal by that of the corresponding signal of a normal 1D spectrum of the same solution. Only the first four data points at low concentrations of the ligand of 29 μM, 56 μM, 82 μM, and 108 μM are showing the exponential decline expected for specific binding. Above these concentrations the specific binding is overlaid by an unspecific binding.

signals from D-Phe Hδ, D-Phe Hε/Hζ, and Val Hγ are shown. During this titration, the intensity of the STD signals increases strongly. The relative STD effect (shown in Figure 4) is defined by dividing the integral of the STD signal by that of the corresponding signal of a normal 1D spectrum. The fraction is expressed as a percentage. The relative STD effect drops even though the absolute intensity of the signal increases with increasing amounts of the ligand. The individual ligand molecules stay in the binding site less frequently and receive less saturation. Only the first four data points at low concentrations of the ligand of 29, 56, 82, and 108 μM show the exponential decline expected for specific binding. Using these data points, a binding constant of about $K_D \approx 30\text{--}60\text{ }\mu\text{M}$ was approximated using a full description of the STD intensities.²⁶ Above these concentrations, the specific binding is overlaid by

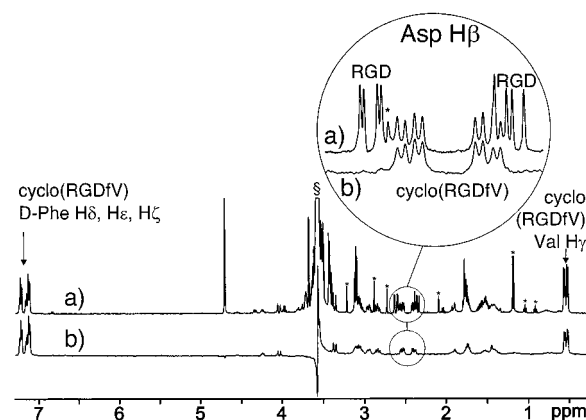


Figure 5. (a) Normal ¹H NMR spectrum of 274 μM RGD and 264 μM cyclo(RGDfV) with integrin α_{IIb}β₃ containing liposomes displaying signals of both ligands. The inset shows the expanded region of the two diastereopic Asp Hβ protons. (S TRIS buffer; * impurity). (b) STD NMR spectrum of 274 μM RGD and 264 μM cyclo(RGDfV) with integrin α_{IIb}β₃ liposomes showing only STD effects of the tight binding cyclopeptide. The inset shows only signals from the tight binding cyclopeptide.

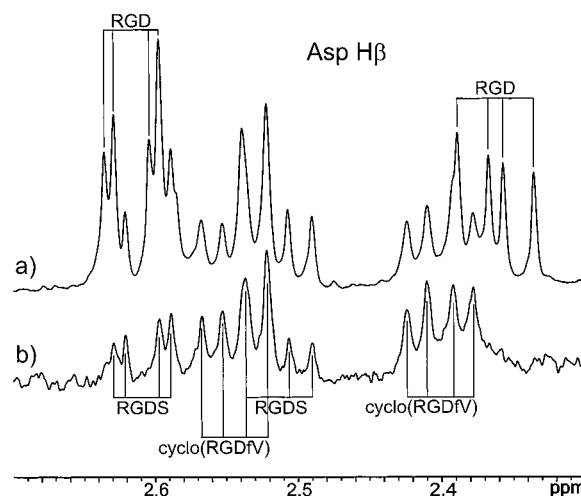


Figure 6. (a) Normal ¹H NMR spectrum of 274 μM RGD, 264 μM cyclo(RGDfV), and 264 μM RGDS with integrin α_{IIb}β₃ liposomes displaying the expanded Asp Hβ signals of all three ligands. (b) STD NMR spectrum of 274 μM RGD, 264 μM cyclo(RGDfV), and 264 μM RGDS with integrin α_{IIb}β₃ liposomes showing only resonances of the tight binding peptides cyclo(RGDfV) and RGDS.

a low-affinity binding. As demonstrated below, this binding mode is not to the liposomes but to the integrin.

Control Experiment with Liposomes Not Containing Integrin. Liposomes without protein were incubated with ligands to integrins to test for the specificity of the effects observed above. Even at concentrations of 260 μM we did not observe any STD effects (cf. Figure 3d). This shows clearly that the peptides do not interact with the liposomes composed of phospholipids only within the lifetime observable by NMR, which is on the low side limited to about 1 ms.

Control Experiments Using Nonbinding Peptides TPL-NH₂ and AGSE. The peptide AGSE (cf. Figure 2) was added up to a concentration of 160 μM to liposomes containing integrin to test for the specificity of the binding. As a result, no STD signals were observed (cf. Figure 3e). In another control experiment, the peptide TPL-NH₂ (cf. Figure 2) was added in a 4-fold

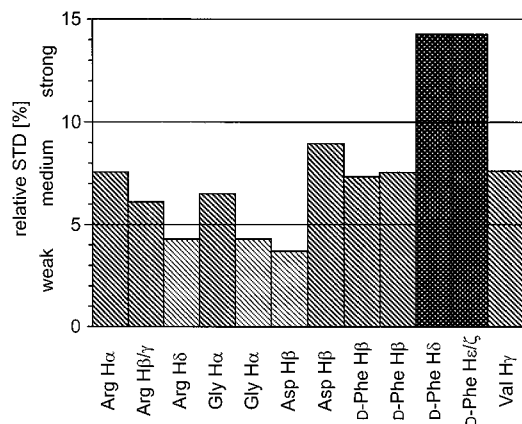


Figure 7. Diagram comparing the STD responses of the individual protons of cyclo(RGDfV) at 30-fold excess of the ligand over the protein. The different intensities in the STD spectrum are classified into weak, medium, and strong STD effects, characterizing the regions with direct saturation transfer as binding epitopes and those with weak signals as receiving saturation only via spin diffusion within the bound ligand.

excess (1.08 mM) to a mixture of liposomes with an equimolar mixture of RGD, cyclo(RGDfV), and RGDS (cf. Figure 2). The signals of TPL-NH₂ could not be observed in the STD spectrum (data not shown). The STD signals of cyclo(RGDfV) and RGDS did not decrease, indicating that TPL-NH₂ does not displace the binding ligands.

Cyclo(RGDfV) is a Competitor of RGD. NMR spectra of integrin containing liposomes with linear RGD and cyclo(RGDfV) gave only STD effects of the stronger binding cyclic peptide (cf. Figure 5). RGD and the cyclopeptide were present in the solution at 130-fold excess to the protein. At this excess, the protein is occupied by the strong ligand at 89.9%. Therefore, RGD has only about 10% of the receptor sites available, and as a consequence its signals do not show up in the STD spectrum due to a lack in intensity. Cyclo(RGDfV) is a more than 34-fold stronger inhibitor of the integrin than RGD (cf. Figure 2). At $K_D = 1$ mM, the peptide RGD would only occupy 20% of the receptor sites left free by cyclo(RGDfV) equivalent to 20 pmol or a concentration of 40 nM, which is far below the detection threshold for the STD system.

RGDS Inhibits the Binding of Cyclo(RGDfV) Partially. Addition of the same amount of the linear

peptide RGDS inhibits the binding of cyclo(RGDfV). Compared to the STD effect of cyclo(RGDfV) before RGDS was added, the signals of the protons Val H γ and D-Phe H δ decreased by 19% and 11%, respectively (spectra not shown). The values of inhibition i are, therefore, 0.19 and 0.11. This fraction expresses the relative decrease of bound ligand displaced by the inhibitor. The formula

$$K_I = \frac{c_i(K_D - iK_D)}{i(c_L + K_D)}$$

K_I \equiv inhibition constant of the added inhibitor RGDS

K_D \equiv dissociation constant of the primary ligand
cyclo(RGDfV)

$c_i = 264 \mu\text{M}$ \equiv concentration of the inhibitor RGDS

$c_L = 264 \mu\text{M}$ \equiv concentration of the ligand
cyclo(RGDfV)

i \equiv inhibition as a fraction

describes the equilibrium binding constant in the case of two ligands competing for one receptor.²⁷ Using a binding affinity of $K_D = 5.05 \mu\text{M}$ for cyclo(RGDfV)¹⁹ and a decrease of 19%, the inhibition constant of RGDS is calculated to be $K_I = 21 \mu\text{M}$; when using a $K_D = 42 \mu\text{M}$ and a decrease of 11%, a $K_I = 293 \mu\text{M}$ results. RGDS shows weaker STD signals than cyclo(RGDfV) (cf. Figure 6) because its resonances receive less saturation due to less available receptor sites when competing with the cyclic peptide.

Epitope Mapping of Cyclo(RGDfV). The STD responses of the individual protons of cyclo(RGDfV) have different intensities in the STD spectrum. This information can be used to assess the binding epitopes of the ligand because protons in close proximity to the protein receptor give more intensive signals than those protons that obtain their saturation only through other ligand protons that in turn have direct contact. The aromatic protons of the D-Phe residue show strong STD effects; a weaker response is observed at the Arg H α , Arg H β /H γ , Asp H β , the β -protons of D-Phe, and the γ -protons of Val, indicating that they together have direct contacts to the integrin (cf. Figure 7). Thus, the binding epitopes of cyclo(RGDfV) were characterized by STD NMR to contain sections of the D-Phe, the Arg H α ,

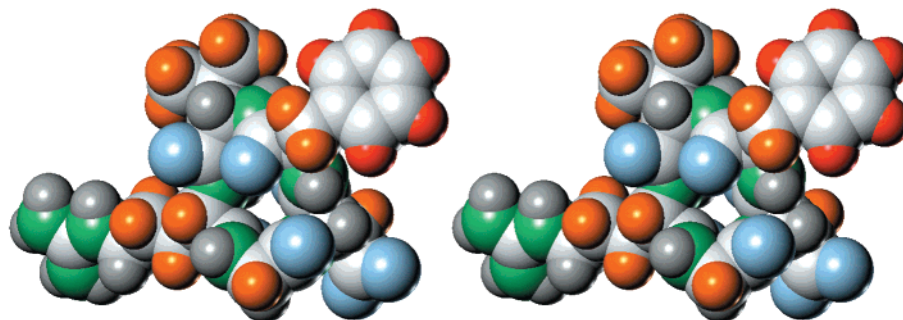


Figure 8. Scheme showing a combination of the 3D structure of cyclo(RGDfV) in DMSO determined by Aumailley et al.¹⁷ (based on NMR spectroscopy and MD simulations) and the STD NMR derived binding epitopes of the cyclic ligand. Nitrogen atoms are shown in green, hydrogen atoms in light gray, carbon atoms in white, and oxygen atoms in blue. The binding epitope is characterized by red colors with those having the tightest contacts to the integrin are shown in red, i.e., the aromatic protons of D-Phe. Those with medium STD intensities are shown in orange, i.e., the H γ of Val, H α , H β , and H γ of D-Phe, one H β of Asp, and one H α of Gly. The red and orange protons together form the binding epitope of cyclo(RGDfV).

H β , and H γ , the Val methyl groups, one α -proton of Gly, and one β -proton of Asp.

Aumailley et al.¹⁷ published a conformation of cyclo-(RGDFV) in DMSO based on 2D NMR spectroscopy and MD simulations, which shows that the side chains of the Arg, Asp, and Val residues are oriented perpendicular to the plane of the cyclic peptide and point to the same side. The side chain of the D-Phe has an approximately equatorial orientation. Combining the information on the binding epitope determined here with the 3D structural information (cf. Figure 8) obtained by Aumailley et al.,¹⁷ the ligand seems to interact with the protein from one side of the peptide ring with the Phe residue in the equatorial plane also making strong contacts. The saturation pattern within the Arg alkyl chain underlines a strongly hydrophobic interaction centered near the backbone. The often postulated ionic interaction of the guanidino group cannot be confirmed because the Arg δ protons show only a very small degree of saturation. This is in agreement with the literature where it was shown that variations of PS-X-GDW that at position X contained the amino acids L-norleucine, L-cyclohexylglycine, L-norvaline, L-*tert*-leucine, or L-4-hydroxyproline²⁸ had higher affinity to $\alpha_{IIb}\beta_3$ than PSRGDW, which suggests little or no contribution of ionic interaction toward the Arg residue.

The strongest STD response originates from the D-Phe phenyl ring. Studying the structure–activity relationship in linear oligopeptide ligands with the general structure RGD-X revealed that the amino acid adjacent to the Asp residue has to have a hydrophobic nature. Hydrophobic and aromatic residues at this position enhanced significantly the inhibitory activity.²⁹ This can also be shown with members of the disintegrin peptide family that are isolated from snake venoms. They effectively inhibit platelet aggregation and often contain the RGDW (but also KGDW or RGDN) amino acid sequence.³⁰ These findings led to the development of highly $\alpha_{IIb}\beta_3$ -specific platelet aggregation inhibitors that are based on the linear amino acid sequence PS-X-GDW³¹ and to the cyclic heptapeptide eptifibatide (Integrilin).^{32,33} The latter contains L-homoarginine in a Har-GDW motif and has gained clinical importance. The structure combines an extended alkyl chain with an aromatic residue adjacent to the RGD analogue sequence and permits stronger hydrophobic interactions. These findings are also in very good agreement with the information on the binding epitope obtained from STD NMR spectroscopy.

Conclusions

The specific binding exerted by the interaction between the RGD peptides analyzed here is overlaid at concentrations of larger than 120 μ M with unspecific binding. It is unclear what mechanism is underlying this effect because no such unspecific binding was found in a ligand/liposome system without integrins present. It is therefore necessary to use as low concentrations as possible to avoid the effects of additional low affinity binding. The STD NMR method could be successfully used to describe the binding epitope of the ligand cyclo-(RGDFV) in full agreement with complementary literature data. This information provides an easy access to the pharmacophore information necessary to optimize the ligands.

Acknowledgment. This work was supported by the DFG through SFB470/B2, Graduate College GRK464, and the BMBF.

References

- (1) Meyer, B.; Weimar, T.; Peters, T. Screening Mixtures for Biological Activity by NMR. *Eur. J. Biochem.* **1997**, *246*, 705–709.
- (2) Haselhorst, T.; Espinosa, J. F.; Jimenez-Barbero, J.; Sokolowski, T.; Kosma, P.; Brade, H.; Brade, L.; Peters, T. NMR Experiments Reveal Distinct Antibody-Bound Conformations of a Synthetic Disaccharide Representing a General Structural Element of Bacterial Lipopolysaccharide Epitopes. *Biochemistry* **1999**, *38*, 6449–6459.
- (3) Mayer, M.; Meyer, B. Mapping the Active Site of Angiotensin-Converting Enzyme by Transferred NOE Spectroscopy. *J. Med. Chem.* **2000**, *43*, 2093–2099.
- (4) Shuker, S. B.; Hajduk, P. J.; Meadows, R. P.; Fesik, S. W. Discovering High-Affinity Ligands for Proteins: SAR by NMR. *Science* **1996**, *274*, 1531–1534.
- (5) Chen, A.; Shapiro, M. J. NOE Pumping. 2. A High-Throughput Method to Determine Compounds with Binding Affinity to Macromolecules by NMR. *J. Am. Chem. Soc.* **2000**, *122*, 414–415.
- (6) Mayer, M.; Meyer, B. Characterization of Ligand Binding by Saturation Transfer Difference NMR Spectroscopy. *Angew. Chem. Int. Ed.* **1999**, *38*, 1784–1788.
- (7) Klein, J.; Meinecke, R.; Mayer, M.; Meyer, B. Detecting Binding Affinity to Immobilized Receptor Protein in Compound Libraries by HR-MAS STD NMR. *J. Am. Chem. Soc.* **1999**, *121*, 5336–5337.
- (8) Mayer, M.; Meyer, B. Group Epitope Mapping (GEM) by STD NMR to Identify Segments of a Ligand in Direct Contact with a Protein Receptor. *J. Am. Chem. Soc.* **2001**, *123*, 6108–6117.
- (9) Hynes, R. O. Integrins: a Family of Cell Surface Receptors. *Cell* **1987**, *48*, 549–554.
- (10) Ruoslahti, E.; Pierschbacher, M. D. New Perspectives in Cell Adhesion: RGD and Integrins. *Science* **1987**, *238*, 491–497.
- (11) Phillips, D. R.; Charo, I. F.; Parise, L. V.; Fitzgerald, L. A. The Platelet Membrane Glycoprotein IIb/IIIa Complex. *Blood* **1988**, *71*, 831–843.
- (12) Albelda, S. M.; Buck, C. A. Integrins and other Cell Adhesion Molecules. *FASEB J.* **1990**, *4*, 2868–2880.
- (13) Pierschbacher, M. D.; Ruoslahti, E.; Sundelin, J.; Lind, P.; Peterson, P. A. The Cell Attachment Domain of Fibronectin. Determination of the Primary Structure. *J. Biol. Chem.* **1982**, *257*, 9593–9597.
- (14) Plow, E. F.; Pierschbacher, M. D.; Ruoslahti, E.; Marguerie, G.; Ginsberg, M. H. Arginyl-Glycyl-Aspartic Acid Sequences and Fibrinogen Binding to Platelets. *Blood* **1987**, *70*, 110–115.
- (15) Kloczewiak, M.; Timmons, S.; Lukas, T. J.; Hawiger, J. Platelet Receptor Recognition Site on Human Fibrinogen. Synthesis and Structure–Function Relationship of Peptides Corresponding to the Carboxy-Terminal Segment of the γ Chain. *Biochemistry* **1984**, *23*, 1767–1774.
- (16) Pierschbacher, M. D.; Ruoslahti, E. Variants of the Cell Recognition Site of Fibronectin That Retain Attachment-Promoting Activity. *Proc. Natl. Acad. Sci. U.S.A.* **1984**, *81*, 5985–5988.
- (17) Aumailley, M.; Gurrath, M.; Müller, G.; Calvete, J.; Timpl, R.; Kessler, H. Arg-Gly-Asp Constrained within Cyclic Pentapeptides. Strong and Selective Inhibitors of Cell Adhesion to Vitronectin and Laminin Fragment P1. *FEBS Lett.* **1991**, *291*, 50–54.
- (18) Haubner, R.; Finsinger, D.; Kessler, H. Stereoisomeric Peptide Libraries and Peptidomimetics for Designing Selective Inhibitors of the $\alpha_v\beta_3$ Integrin for a New Cancer Therapy. *Angew. Chem. Int. Ed.* **1997**, *36*, 1374–1389.
- (19) Pfaff, M.; Tangemann, K.; Müller, B.; Gurrath, M.; Müller, G.; Kessler, H.; Timpl, R.; Engel, J. Selective Recognition of Cyclic RGD Peptides of NMR Defined Conformation by $\alpha_{IIb}\beta_3$, $\alpha_v\beta_3$, and $\alpha_5\beta_1$ Integrins. *J. Biol. Chem.* **1994**, *269*, 20233–20238.
- (20) Keenan, R. M.; Miller, W. H.; Kwon, C.; Ali, F. E.; Callahan, J. F.; Calvo, R. R.; Hwang, S. M.; Kopple, K. D.; Peishoff, C. E.; Samanen, J. M.; Wong, A. S.; Yuan, C. K.; Huffman, W. F. Discovery of Potent Nonpeptide Vitronectin Receptor ($\alpha_v\beta_3$) Antagonists. *J. Med. Chem.* **1997**, *40*, 2289–2292.
- (21) Gerritsen, W. J.; Verkley, A. J.; Zwaal, R. F.; Van Deenen, L. L. Freeze-Fracture Appearance and Disposition of Band 3 Protein From the Human Erythrocyte Membrane in Lipid Vesicles. *Eur. J. Biochem.* **1978**, *85*, 255–261.
- (22) Müller, B.; Zerwes, H. G.; Tangemann, K.; Peter, J.; Engel, J. Two-Step Binding Mechanism of Fibrinogen to $\alpha_{IIb}\beta_3$ Integrin Reconstituted into Planar Lipid Bilayers. *J. Biol. Chem.* **1993**, *268*, 6800–6808.
- (23) Holloway, P. W. A Simple Procedure for Removal of Triton X-100 from Protein Samples. *Anal. Biochem.* **1973**, *53*, 304–308.

- (24) Erb, E. M.; Tangemann, K.; Bohrmann, B.; Müller, B.; Engel, J. Integrin $\alpha_{IIb}\beta_3$ Reconstituted into Lipid Bilayers is Non-clustered in its Activated State but Clusters after Fibrinogen Binding. *Biochemistry* **1997**, *36*, 7395–7402.
- (25) Mimms, L. T.; Zampighi, G.; Nozaki, Y.; Tanford, C.; Reynolds, J. A. Phospholipid Vesicle Formation and Transmembrane Protein Incorporation Using Octyl Glucoside. *Biochemistry* **1981**, *20*, 833–840.
- (26) Meyer, B.; et al. Unpublished results.
- (27) Cantor, C. R.; Schimmel, P. R. In *Biophysical Chemistry*; W. H. Freeman and Company: New York, 1980; p 943.
- (28) Hayashi, Y.; Katada, J.; Sato, Y.; Igarashi, K.; Takiguchi, Y.; Harada, T.; Muramatsu, M.; Yasuda, E.; Uno, I. Discovery and Structure–Activity Relationship Studies of a Novel and Specific Peptide Motif, Pro-X-X-X-Asp-X, as a Platelet Fibrinogen Receptor Antagonist. *Bioorg. Med. Chem.* **1998**, *6*, 355–364.
- (29) Tranqui, L.; Andrieux, A. H.-C., G.; Ryckewaert, J.-J.; Soye, S.; Chapel, A.; Ginsberg, M. H.; Plow, E. F.; Marguerie, G. Differential Structural Requirements for Fibrinogen Binding to Platelets and to Endothelial Cells. *J. Cell Biol.* **1989**, *108*, 2519–2527.
- (30) Scarborough, R. M.; Rose, J. W.; Naughton, M. A.; Phillips, D. R.; Nannizzi, L.; Arfsten, A.; Campbell, A. M.; Charo, I. F. Characterization of the Integrin Specificities of Disintegrins Isolated from American Pit Viper Venoms. *J. Biol. Chem.* **1993**, *268*, 1058–1065.
- (31) Katada, J.; Hayashi, Y.; Sato, Y.; Muramatsu, M.; Takiguchi, Y.; Harada, T.; Fujiyoshi, T.; Uno, I. A Novel Peptide Motif for Platelet Fibrinogen Receptor Recognition. *J. Biol. Chem.* **1997**, *272*, 7720–7726.
- (32) Scarborough, R. M.; Naughton, M. A.; Teng, W.; Rose, J. W.; Phillips, D. R.; Nannizzi, L.; Arfsten, A.; Campbell, A. M.; Charo, I. F. Design of Potent and Specific Integrin Antagonists. Peptide Antagonists with High Specificity for Glycoprotein IIb-IIIa. *J. Biol. Chem.* **1993**, *268*, 1066–1073.
- (33) Phillips, D. R.; Scarborough, R. M. Clinical Pharmacology of Eptifibatide. *Am. J. Cardiol.* **1997**, *80*, 11B–20B.

JM0109154